

## Rapid Communications

*Rapid Communications are intended for the accelerated publication of important new results and are therefore given priority treatment both in the editorial office and in production. A Rapid Communication in Physical Review B should be no longer than four printed pages and must be accompanied by an abstract. Page proofs are sent to authors.*

### Equilibrium point defects in intermetallics with the *B2* structure: NiAl and FeAl

C. L. Fu, Y.-Y. Ye,\* and M. H. Yoo

*Metals and Ceramics Division, Oak Ridge National Laboratory, Oak Ridge, Tennessee 37831-6114*

K. M. Ho

*Ames Laboratory and Department of Physics, Iowa State University, Ames, Iowa 50011*

(Received 11 June 1993)

Equilibrium point defects and their relation to the contrasting mechanical behavior of NiAl and FeAl are investigated. For NiAl, the defect structure is dominated by two types of defects—monovacancies on the Ni sites and substitutional antisite defects on the Al sites. The defect structure of FeAl differs from that of NiAl in the occurrence of antisite defects at the transition-metal sites for Al-rich alloys and the tendency for vacancy clustering. The strong ordering (and brittleness) of NiAl is attributed mainly to the difference in atomic size between constituent atoms.

Ordered intermetallics have already been established as an important class of high-temperature structural materials. The crystal structure of the *B2* (CsCl) type is one of the simplest and most common ordered structures. Yet, *B2*-type intermetallics exhibit some of the most interesting and diverse physical phenomena in alloys.<sup>1</sup> One outstanding example is the contrasting mechanical behavior of NiAl and FeAl. These two aluminides differ not only in their deformation and fracture behavior,<sup>1,2</sup> but also in their mechanical response to thermomechanical processing.<sup>3-5</sup> NiAl is known to be a strongly ordered but brittle system. FeAl is relatively ductile but its physical properties are sensitive to extrinsic defects<sup>6</sup> as well as to the thermomechanical history.<sup>3-5</sup> Among other quantities, the lattice defects are often thought to play major roles in the mechanical behavior of these alloys. For example, the fact that the hardness of FeAl has a strong dependence on the cooling rate implies that quenched-in vacancies are more prevalent in FeAl than in NiAl. Although point defect structure in intermetallics has been studied extensively by various experimental techniques, fundamental information on the temperature and composition dependence of point defect properties is still not fully available. Theoretical efforts to calculate the point defects in aluminides have been limited to models using nearest-neighbor pair-wise interactions<sup>7</sup> or embedded-atom potentials.<sup>8</sup> While these have provided useful insights, the calculation of point defect properties remains a challenging problem, because both the atomic size and electronic structure effects are expected to play significant roles. In this paper, we present results from a local-density-functional (LDF) study of the point defect properties in NiAl and FeAl. The point defect structure in NiAl is dominated by two types of defects—monovacancies on the Ni sites and substitutional antisite

defects on the Al sites. For FeAl, on the other hand, a more complex defect structure is found and a strong tendency for vacancy clustering is predicted. Our investigation shows that a comprehensive understanding of the lattice defects forms the basis for a better assessment of various mechanical behavior in ordered intermetallics (such as ordering and slip behavior, ductility and strength, and microhardness variation).

The constitutional point defects in NiAl were investigated experimentally by Bradley and Taylor<sup>9</sup> as early as in 1937. They concluded that the defects are vacancies in Al-rich alloys and antisite defects in Ni-rich alloys. Later experiments have more or less confirmed their results, although the measured vacancy formation energies are widely scattered. Very recently, the defect structure in NiAl was identified, using perturbed angular correlation of gamma rays, to be Schottky type (with vacancies on both sublattices) with a formation energy of 2.66 eV.<sup>10</sup> Clearly, the detailed defect information is still incomplete even for the well-studied case of NiAl. FeAl is known to retain a high concentration of thermal vacancies for samples quenched from high temperatures.<sup>3-5,11</sup>

In this investigation a supercell approach is used to describe the energies of an isolated point defect. In this regard, two supercell geometries are employed to examine the convergence of point defect energies with respect to the supercell size: a single defect within a 16-atom supercell (with defects forming a simple cubic Bravais lattice), and a single defect within a 32-atom supercell (with defects forming a fcc Bravais lattice). The LDF equations are solved self-consistently by use of the mixed-basis pseudopotential method.<sup>12</sup> Relaxed defect geometries are optimized by calculating forces<sup>13</sup> acting on the atoms using the Hellmann-Feynman theorem. The electronic wave functions are expanded in a mixed basis set with

five localized  $d$  orbitals per atom (for Ni and Fe) in a numerical form and plane waves with a cutoff energy of 12.5 Ry. The lattice constants used in this investigation are determined from total-energy calculations at stoichiometry, which have calculated values of 2.84 Å and 2.80 Å for NiAl and FeAl, respectively.

NiAl and FeAl have similar lattice constants. But, they have very different mechanical behavior. For example, the primary deformation mode of NiAl is  $\langle 100 \rangle$  slip, whereas FeAl shows normal  $\langle 111 \rangle$  slip behavior;<sup>1</sup> the cleavage habit plane is reported to be (110) for NiAl, but a (100) plane is observed for FeAl.<sup>14</sup> Our calculation shows that FeAl and NiAl are also dissimilar in bonding characteristics. The calculated density of states of  $B2$  aluminides is distinguished by a "pseudogap" separating the bonding (between transition metals and aluminum) and nonbonding states. In FeAl, the electronic state has an unfilled  $d$  shell and the Fermi level ( $E_F$ ) lies in the Fe-Al bonding state region. Thus, the bonding strength (and mechanical behavior) is very sensitive to intrinsic and extrinsic defects. By contrast, NiAl has a more closed  $d$  shell and the Ni-Al bonding states are well below  $E_F$ .

In our approach to calculating the point defect structure, we assume the defects are sufficiently dilute that their interactions can be neglected and we consider only the configurational part of the entropy term. The defect concentrations are then determined from the minimization of the grand potential  $\Omega$ . We adopted the approach of using a fixed number of lattice sites, but allowing the total number of atoms to be variable (and the ratio of the numbers of  $A$  atoms to  $B$  atoms for an  $AB$  compound should satisfy a given stoichiometry). Thus, a generalized function  $\Omega^*$  can be constructed for the purpose of minimization, i.e.,

$$\Omega^* = \Omega - L_\alpha (M^\alpha - N_V^\alpha - N_A^\alpha - N_B^\alpha) - L_\beta (M^\beta - N_V^\beta - N_A^\beta - N_B^\beta), \quad (1)$$

for a system with two different sites (i.e.,  $A$  atoms in the  $\alpha$  sites and  $B$  atoms in the  $\beta$  sites for a perfect crystal). In Eq. (1),  $L_\alpha$  and  $L_\beta$  are Langrangian multipliers,  $M^\alpha$  is the number of sites for component  $\alpha$ , and  $N_V^\alpha$ ,  $N_A^\alpha$ , and  $N_B^\alpha$  are the number of vacancies,  $A$  atoms, and  $B$  atoms at site  $\alpha$ , respectively (similar expressions are for the  $\beta$  sites). The enthalpy of the system is evaluated from first principles at 0 K in the presence of the noninteracting defects. The minimization of  $\Omega^*$  with respect to the number of defects leads to the following expressions for point defect concentrations (referred to the total number of lattice sites) at site  $\alpha$  in thermal equilibrium:

$$n_V^\alpha = \frac{1}{2} \left[ \frac{e^{-(E_V^\alpha + \mu_A)/k_B T}}{1 + e^{-(E_V^\alpha + \mu_A)/k_B T} + e^{-[E_B^\alpha - (\mu_B - \mu_A)]/k_B T}} \right] \quad (2)$$

and

$$n_B^\alpha = \frac{1}{2} \left[ \frac{e^{-[E_B^\alpha - (\mu_B - \mu_A)]/k_B T}}{1 + e^{-(E_V^\alpha + \mu_A)/k_B T} + e^{-[E_B^\alpha - (\mu_B - \mu_A)]/k_B T}} \right], \quad (3)$$

where  $E_V^\alpha$  and  $E_B^\alpha$  are the internal energies of a vacancy and an antisite defect at site  $\alpha$  and  $\mu_A$  and  $\mu_B$  are the chemical potentials for atoms  $A$  and  $B$ , respectively, which are determined through a set of nonlinear equations obtained from the grand canonical ensemble (as described above).

We first consider the point defects in NiAl. Among four kinds of point defects (i.e., substitutional antisites and structural vacancies on both sublattices), we only find the presence of two kinds of defects for NiAl at stoichiometry, i.e., substitutional antisite defects on the Al sublattice and structural vacancies on the Ni sublattice. The defect concentration as a function of temperature is shown in an Arrhenius plot (cf. Fig. 1). The vacancy concentration on the Ni sublattice at high temperature (above 1000°C) is found to be  $10^{-3}$ – $10^{-4}$ , which is in good agreement with experiments.<sup>7</sup> The effective vacancy formation energy at the Ni sites is 0.93 eV and the formation energy for antisite defect at the Al sites is 0.97 eV. At stoichiometry, we find that the point defect configuration for NiAl is of triple-defect type, i.e., two well-separated monovacancies at the Ni sites accompanied by an antisite defect at the Al sites. Other kinds of defect configuration (e.g., Schottky defects) are found to be unstable due to higher defect formation energies (cf. Table I) associated with antisite defects at the Ni sites and vacancies at the Al sites. (The results reported here have been obtained using the 32-atom supercell geometry and are basically identical to those obtained from the 16-atom supercell. For example, the vacancy formation energies differ by less than 0.05 eV between these two cases.)

In sharp contrast to the point defect structure in close-packed lattices and in most known  $B2$  alloy systems

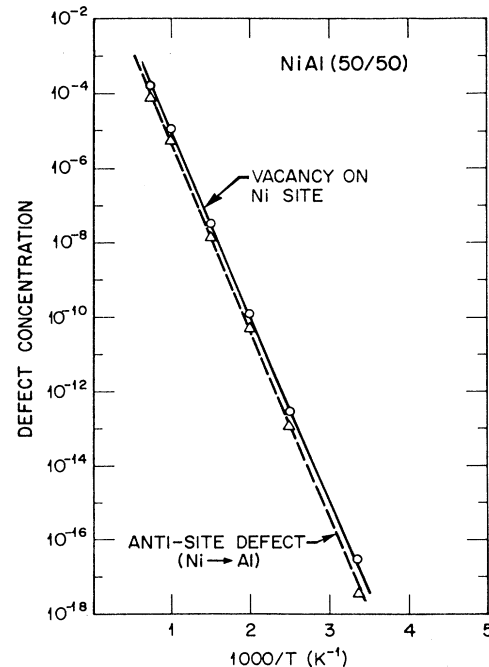


FIG. 1. Arrhenius plot for point defect concentration of NiAl at stoichiometry.

TABLE I. Point defect formation energies (in eV) of NiAl and FeAl at stoichiometry.  $E_V(A)$  and  $E_{\text{anti}}(A)$  are the vacancy and antisite formation energies at  $A$ -atom sites, respectively. TM is the abbreviation for transition metal.

	$E_V(\text{TM})$	$E_V(\text{Al})$	$E_{\text{anti}}(\text{TM})$	$E_{\text{anti}}(\text{Al})$
NiAl	0.93	2.14	2.18	0.97
FeAl	0.97	4.00	1.03	0.95

(with lower ordering temperature), the point defect configuration for off-stoichiometric NiAl is drastically different for Ni-rich and Al-rich cases. As shown in Fig. 2, the dominant point defect types found in our calculation are (1) substitutional antisite defects at the Al sublattices for the Ni-rich side and (2) structural vacancies at the Ni sublattices for the Al-rich side. Furthermore, we find that there is an abrupt change in the vacancy and antisite concentrations around stoichiometry. At high temperatures (cf. Fig. 2), however, there still exists a residual vacancy concentration at the Ni sites (about  $10^{-5}$ ) for Ni-rich NiAl; there is a two order of magnitude difference between vacancy and antisite defect concentrations for Al-rich NiAl. We do not find the presence of thermal vacancies at the Al sublattices even at high temperatures (for which the concentration is about  $10^{-20}$ ). Thus, our calculation rules out the existence of Shottky defects in NiAl due to the high formation energy of vacancies at the Al sublattices. The preference of substitutional antisites defects over vacancies at the Al sites demonstrates the fact that metallic bonding is a favorable bonding mode among Ni atoms once they are in nearest-neighbor proximity. On the other hand, since Al has a larger atomic radius than Ni, structural vacancies are preferred over antisite defects at the Ni sublattice for Al-rich NiAl so that nearest-neighbor Al-Al repulsion can

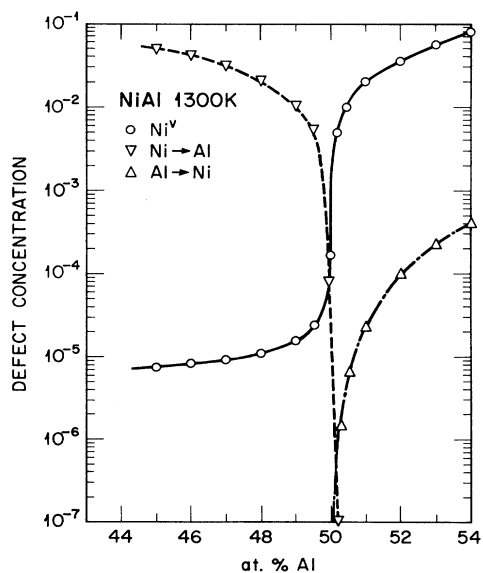


FIG. 2. The dependence of point defect configuration of NiAl on atomic percentage of Al at 1300 K.  $\text{Ni}^V$  stands for vacancies at the Ni sites.  $A \rightarrow B$  indicates that a  $B$  atom is replaced by an  $A$  atom.

be avoided, if the difference in atomic size is a dominant effect.

Now consider the point defects in FeAl. Similar to the case of NiAl, low monovacancy formation energy at the Fe sites (0.97 eV) and low antisite defect formation energy at the Al sites (0.95 eV) are found for FeAl at stoichiometry. However, a basic difference between these two alloys is found in the antisite formation energy at the transition-metal (TM) sites (cf. Table I). For FeAl, we find a relatively low antisite formation energy at the Fe sites with a value of 1.04 eV at stoichiometry. Clearly, other than the atomic size effect, the electronic structure effect is an important factor in determining the point defect structure of FeAl. (Since FeAl has partially unfilled Fe-Al bonding states, the local Fe-Al bonding can be enhanced near the antisite defect sites, where Fe atoms are replaced by more electropositive elements, such as Al in FeAl, i.e., a mechanism similar to that of  $d$ -band filling through the  $d$ - $p$  hybridization effect proposed for Ni and Pd alloys.<sup>15</sup>) Indeed, as shown in Fig. 3, for the concentration of point defects at high temperatures, there is competition between vacancies and antisite defects at the Fe sublattice. In fact, the substitutional antisite defects at the Fe sites become the dominant defect type for Al-rich FeAl.<sup>16</sup> For Fe-rich FeAl, on the other hand, the constitutional antisite defect at the Al sites is the main defect type—as in the case of NiAl. Also similar to NiAl, we do not find the presence of vacancies at the Al sublattices. A vacancy concentration of  $10^{-4}$  at the Fe sites is obtained at stoichiometry for FeAl at 1300 K. This value is too low by two orders of magnitude compared with the experimental data in the literature.<sup>4,5,11</sup> However, it should be noted that the calculation simulates a thermal equilibrium condition (which corresponds

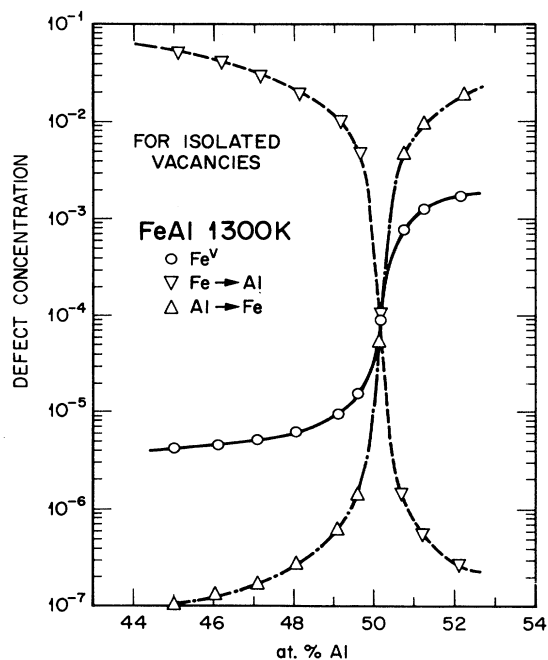


FIG. 3. The dependence of point defect configuration of FeAl on atomic percentage of Al at 1300 K near stoichiometry (based on noninteracting defect model). See Fig. 2 for notations.

to sufficiently long annealing time) under the assumption that the defects are well separated (i.e., large vacancy clusters can be annealed out by forming, for example, faulted dislocation loops<sup>4</sup>). Thus, in order to rationalize the difference between the present calculation and experiments, and to understand the strong dependence of hardness on heat treatment for FeAl, we have to examine the possibilities of defect clustering and complexes.

Among various kinds of point defects in FeAl, we find that the vacancy formation energy at the Fe sites has a stronger dependence on the supercell size as compared to other types of defects, i.e., the vacancy formation energy increases as the distance between vacancies increases. To investigate the interaction between vacancies, we consider the case of divacancies, in which two vacancies at the Fe sites are separated by the distance of a lattice constant. The binding energy of divacancies is then determined by comparing the defect self-energies of monovacancies and divacancies. Our calculation indicates that divacancies in FeAl have a significantly high binding energy (i.e., attractive) with a value of 0.57 eV. The implications of our results are (1) there is a strong tendency for vacancy clustering and (2) the vacancies can be annealed out to open structures, such as dislocations, voids, or grain boundaries. Since microhardness is related to the defect concentration (in particular, vacancies) and the lattice distortion associated with defects, it is not surprising that the microhardness of FeAl shows strong dependence on the thermomechanical treatment.<sup>3-5</sup> By contrast, with the similar calculation applied to NiAl, we find that the interaction between vacancies tends to be weakly repulsive with a divacancy binding energy of -0.1 eV. Thus, a monovacancy configuration is a stable defect structure in NiAl and its related mechanical properties are far less sensitive to the thermal annealing time.<sup>3</sup> Our calculation correctly explains the contrasting mechanical behavior between NiAl and FeAl with respect to the cooling rate of the samples.

For both NiAl and FeAl, larger lattice distortions are found for defects in Al-rich alloys. For antisite defects at the Fe sites, there is a 4% outward and 1.5% inward relaxation for atoms on the first and second atomic shells around the defect sites, respectively, with respect to the

interatomic distances of the defect-free lattice. For vacancies at the TM sites, the relaxations are 1% inward and about 1% outward for surrounding atoms on the first and second atomic shells, respectively, in both NiAl and FeAl. By contrast, the lattice relaxations associated with the antisite defects at the Al sites, which is the major defect type in TM-rich alloys, are relatively small (i.e., less than 1% inward relaxation for atoms on the first atomic shell). Our results (i.e., higher vacancy concentration and larger lattice distortions for antisite defects at the TM sites in Al-rich alloys) correlate well with the observation that the composition dependence of off-stoichiometric hardening is steeper on the Al-rich side than on the TM-rich side.<sup>3,5</sup>

We have shown that a major difference in the point defect structure between NiAl and FeAl is the absence of substitutional antisite defects at the TM sites in NiAl (i.e., Al atoms avoid other Al atoms as their nearest neighbor in NiAl). One consequence of this ordering behavior is that  $\langle 111 \rangle$  slip should be prohibited in NiAl, since a  $\frac{1}{2}\langle 111 \rangle$  partial slip necessarily brings the same type of atoms into nearest-neighbor contact. Thus, it is not entirely unexpected that NiAl shows anomalous  $\langle 100 \rangle$  slip, which is also a common feature observed in other B2-type alloys with high ordering temperature (e.g., CoAl, AuZn, NiGa, etc.). As a consequence of having  $\langle 100 \rangle$  slip, the brittleness of NiAl has been associated with the lack of independent slip systems for slip deformation. The strong ordering (and brittleness) of NiAl is attributed mainly to the difference in atomic size between constituent atoms. On the other hand, FeAl is observed to have  $\langle 111 \rangle$  slip, which is closely related to the fact that the substitutional antisite defects can be equilibrium point defects on both sublattices in FeAl.

Research at ORNL was sponsored by the Division of Materials Science, Office of Basic Energy Sciences, U.S. Department of Energy under Contract No. DE-AC05-84OR21400 with Martin Marietta Energy Systems, Inc. Ames Laboratory is operated for the U.S. Department of Energy by Iowa State University under Contract No. W-7405-Eng-82.

\*Present address: Dept. of Materials Science and Engineering, University of Tennessee, Knoxville, Tennessee.

<sup>1</sup>I. Baker and P. R. Munroe, in *High Temperature Aluminides & Intermetallics*, edited by S. H. Whang, C. T. Liu, D. P. Pope, and J. O. Stiegler (The Minerals, Metals and Materials Society, Warrendale, PA 1990), p. 425, and references cited therein.

<sup>2</sup>C. L. Fu and M. H. Yoo, *Acta Metall.* **40**, 703 (1992).

<sup>3</sup>P. Nagpal and I. Baker, *Metall. Trans.* **21A**, 2281 (1990).

<sup>4</sup>D. Weber, M. Meurtin, D. Paris, A. Fourdeux, and P. Lesbats, *J. Phys. C* **7**, 332 (1977).

<sup>5</sup>Y. A. Chang, L. M. Pike, C. T. Liu, A. R. Bilbrey, and D. S. Stone, *J. Intermetall.* **1**, 107 (1993).

<sup>6</sup>C. T. Liu, E. H. Lee, and C. G. McKamey, *Scr. Metall.* **23**, 875 (1989).

<sup>7</sup>P. Neumann, Y. A. Chang, and C. M. Lee, *Acta Metall.* **24**,

593 (1976), and references cited therein.

<sup>8</sup>S. M. Foiles and M. S. Daw, *J. Mater. Res.* **2**, 5 (1987).

<sup>9</sup>A. J. Bradley and A. Taylor, *Proc. R. Soc. A* **159**, 56 (1937).

<sup>10</sup>J. Fan, Ph.D. dissertation, Washington State University, 1991.

<sup>11</sup>H. Lafi, M. Dirand, L. Bourden, J. Hertz, D. Weber, and P. Lesbats, *Acta. Metall.* **34**, 425 (1986).

<sup>12</sup>S. G. Louie, K. M. Ho, and M. L. Cohen, *Phys. Rev. B* **19**, 1774 (1979).

<sup>13</sup>K. M. Ho, C. L. Fu, and B. N. Harmon, *Phys. Rev. B* **29**, 1575 (1984).

<sup>14</sup>M. H. Yoo and C. L. Fu, *Scr. Metall.* **25**, 2345 (1991).

<sup>15</sup>J. C. Fuggle, F. U. Hillebrecht, R. Zeller, Z. Zolnieriek, and P. A. Bennett, *Phys. Rev. B* **27**, 2145 (1983).

<sup>16</sup>Note that the antisite defects at the Fe sites are constitutional defects for Al-rich FeAl and the vacancies at the Fe sites are thermal vacancies in this case.